Modelling of Gas and Slurry Phase Polyolefin Production: The importance of thermodynamics

Duarte Morais Ceclio
duarte.cecilio@tecnico.ulisboa.pt

Instituto Superior Técnico, Lisboa, Portugal

October 2015

Abstract

This thesis studies the effect of polymer swelling in polyethylene production by slurry and gas-phase processes. The work comprises the development of two different models. The first one calculates the Particle Size Distribution (PSD) of polyethylene produced in slurry phase, and studies the impact of polymer swelling on the corresponding PSD. The second model describes the operation of a gas-phase HDPE reactor in dry mode and investigates the influence of the addition of an inert alkane, on polymer swelling and on HDPE production. The first developed model predicts the PSD of a polyethylene for a reactor train of n CSTRs. The simulations performed calculate the PSD of the polymer exiting the 2nd reactor. Parameters like, catalyst size and diluent type were analyzed. From the results it is possible to conclude that diluent type greatly affects monomer concentration and therefore polymer swelling. In the second part of the work, a gas-phase polyethylene process is studied in dry mode operated fluidized bed reactors. The developed model predicts the steady-state polyethylene production and the reactor operating conditions. Effective ethylene concentrations near the catalyst active sites were predicted using the Sanchez-Lacombe EOS thermodynamic model. The model was validated with data gathered from Patent US 6864332 B2. From the results it is possible to conclude that, for the same partial pressure, adding n-hexane yields higher productions over adding isobutane. However, component vapor pressure indicates that it is possible to add greater quantities of isobutane while maintaining dry mode operation, thus achieving higher overall productions.

Keywords: Polyethylene PSD, Polymer swelling, Gas-phase Polyethylene Production, FBR Reactor Modelling, Dry Mode

1. Introduction

In the family of polyolefins, polyethylene is one of its most important members. Different types of polyethylenes, divided according to a specific property. When this property is density, polyethylene is divided into: High Density Polyethylene (HDPE), Low Density Polyethylene and Linear Low Density Polyethylene (LLDPE). While HDPE is a made of highly linear unbranched molecules, LDPE and LLDPE present different degrees of branching, where the concentration of branching is higher in LDPE and slightly lower in LLDPE. The result is density varying from 0.94 to 0.97 g/cm^3 for HDPE and 0.90-0.94 g/cm^3 for LDPE and LLDPE [8].

Polyethylene is the most widely produced polymer in the world, presenting a 78 million tonne demand in 2012, which corresponds to 37% of worldwide polymer demand in said year. Predictions indicate that polyethylene demand will increase at least until 2017 [13].

It is such context that this work comes into light. Polyethylene is part of a high volume market and further development is of the utmost interest.

The objective of this work is to study the impact of polymer swelling in slurry and gas phase polyethylene procution. In slurry phase this will be achieved through the development of a model to predict the polymer's PSD. In gas-phase this will be achieved through the development of a model to describe the production and behaviour of an FBR reactor operating in *dry* mode.

2. Background

There are three different types of processes for catalytic olefin polymerization: solution, slurry or gas-phase. Solution processes rely on an homogeneous catalyst and are used to produce Ethylene Propylene Diene Monomer rubbers. The reactors used are typically stirred autoclaves, operating at temperatures ranging from 150 to 250°C. However, this type of processes is not considered in this work.

Slurry and gas-phase processes have one similarity: the polymer is formed around heterogeneous catalyst particles.

Slurry processes are subdivided into diluent and

bulk. Diluent processes use a liquid heavy alkane (C_4 to C_6) to suspend the particles while gaseous and/or liquid monomer is fed. The bulk process uses liquid propylene, so it is only possible to produce polypropylene. Slurry processes employ reactor such as the autoclave, loop reactor or CSTR. Gas-phase processes make use of the FBR or stirred bed reactors, although only the FBR is employed in industry [10].

2.1. Particle Fragmentation and Growth

Supported catalyst particles, such as the widely used Ziegler-Natta catalysts, are highly porous secondary particles, formed by aggregated primary particles.
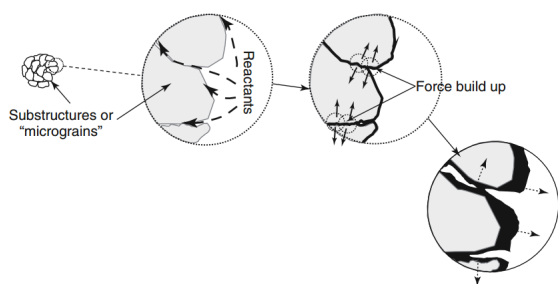

Figure 1: Particle growth evolution [10].

During polymerization the inorganic phase of the particles suffers a build-up of stress at the weak points where the primary particles are in contact, as shown in figure 1. The particles then fragment due to the growth of the polymer chains and result in expanding polymer particles, consisting of primary particles, living chains and dead chains [10].

If no problems occur during polymerization and fragmentation, the result is that the PSD of the polymer after polymerization is similar to the PSD of the catalyst before undergoing polymerization. This is called the replication phenomenon.

One crucial aspect related to polymerization in heterogeneous catalysts is that the rate of polymerization depends on the concentration of active sites on the surface of the micrograins and on the monomer concentration at the active sites. Therefore the monomer must solubilize and diffuse through the growing polymer phase to reach the active sites located on the surface of the micrograins. However, it can only solubilize in the amorphous phase of the polymer, as opposed to the crystalline phase.

2.2. Slurry Phase Processes

Slurry phase processes include 3 phases inside the reactor: a gas-phase, containing the ethylene, hydrogen and possibly comonomer, and a slurry containing solid catalyst and polymer particles and the liquid diluent.

The first commercial slurry process used a series of CSTR to compensate for low catalyst activity. A deashing operation was also needed to remove catalyst residue. Advances in catalyst technology makes it possible to achieve the same results in two reactors without deashing, nowadays.

The following image (figure 2) shows an example of the Hostalen process by LyondelBasell, to explain slurry processes in further detail.
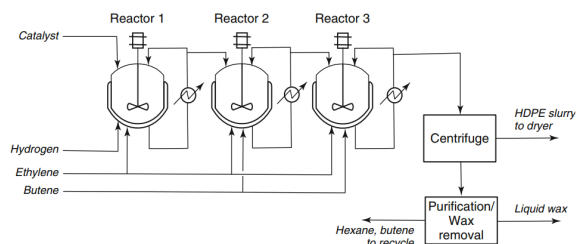

Figure 2: Simplified scheme of the new Hostalen process from LyondellBasell [10].

The Hostalen process makes use of the three reactor configuration. The reactors are stirred autoclaves and can be operated in series or in parallel. When operated in series the monomer is only fed to the first reactor and the result is an increase in production. The advantage of parallel operation is the ability to produce different poylmers [10].

On the first reactor a catalyst with a decay profile is added, producing a low molecular weight homopolymer. Since hydrogen (controls molecular weight as a chain transfer agent) causes a decrease in polymerization rate, it must be added when the catalyst shows its highest intrinsic activity (hence, the first reactor).

In the second and sometimes third reactors a small amount of an -olefin comonomer is introduced. This increases the rate of reaction, regarding homopolymerization, and maintaining good productivity. This is referred to as the co-monomer kick [10].

2.3. Gas-Phase Processes

Gas-phase polyethylene production processes rely solely on fluidized bed reactors. Their main advantage is the gaseous reaction medium, thus making monomer separation easier. The low weight polymer formed remains attached to the polymer particles, rendering further separations unnecessary. As such, gas-phase processes are true swing processes. In other words, they can be used to produce resins from the LLDPE grade to the HDPE grade in the same process [10].

The following figure 3 represents a simplified

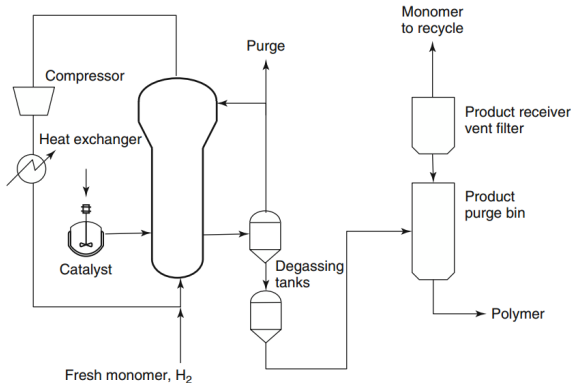scheme of a polymerization plant with a fluidized bed reactor.

Figure 3: Unipol process for polyethylene production [10].

Fresh monomer and hydrogen are fed to the reactor as well as fresh catalyst. There is a product discharge valve to remove the polymer, degassing tanks to separate the unreacted monomer and a purge column to remove any residual monomer and deactivate the catalyst. The recovered unreacted monomer is compressed, heated and afterwards mixed with the fresh monomer and recycled to the reactor. These first generation plants presented frequent reactor runaway issues but improvements in catalyst technology and process control systems rendered these issues almost nonexistent. Modern plants can also be operated in condensed mode, increasing throughput [10].

Ziegler-Natta and metallocene catalysts require an additional prepolymerization step. This step serves two purposes: to maintain particle morphology and, more importantly, to prevent particle overheating and polymer melting.

2.3.1 Fluidized Bed Reactors

The Fluidized Bed Reactor is divided into three zones: the distributor plate, the reaction zone and the disengagement zone.

The distributor plate appropriately distributes the components in the powder bed. The holes in the plate allow the passage of the gases and possible liquid droplets while preventing the settling of of particles in the injection zone. The reaction zone begins above the distributor plate and ends at the freeboard zone. The latter is where void fraction is close to 1 and particle's velocity decreases below minimum fluidization velocity, causing them to fall back into the powder bed. To account for some fines generation the diameter of the disengagement zone is doubled.

One of the most important obstacles to increase polyethylene production nowadays is heat removal, due to the significant catalyst advances made in recent decades as well as the exothermicity of polymerization reactions. To increase heat removal an inert heavy alkane is introduced in the gas stream, effectively increasing its heat capacity. The reactor can then be operated either in dry mode or in condensed mode.

In dry mode operation the purpose is to transfer the heat to the gas phase, according to the following equation.

$$\Delta H_g = Q_m \cdot C_p \left(T_{out} - T_{in}\right) \qquad (1)$$

where ΔH_g is the heat that the gaseous stream is able to remove, Q_m is the stream's mass flowrate, C_p its heat capacity and $(T_{out} - T_{in})$ the temperature gradient between outlet and inlet. Typically C_4 to C_6 alkanes are preferred.

In condensed mode operation the reactor outlet stream is cooled below the dew point of the heavy alkane, resulting the partial condensation of the recycle stream, which is the fed into the reactor. As it is introduced it vaporizes, removing more polymerization heat. Apart from an inert heavy alkane a comonomer can also be used as condensable material. This material is referred to as Induced Condensing Agent or Inert Condensing Agent.

2.4. Sanchez-Lacombe EOS

The Sanchez-Lacombe EOS was used to predict the solubility of the monomer in the polymer phase. It takes the following form.

$$\overline{\rho}^2 + \overline{P} + \overline{T} \left[\ln(1 - \overline{\rho}) + \left(1 - \frac{1}{r}\right) \overline{\rho}\right] = 0 \qquad (2)$$

where $\overline{\rho}, \overline{P}, \overline{T}$ are the reduced density, pressure and temperature, respectively. Sanchez-Lacombe EOS is a widely used thermodynamic model in the polyolefin industry since its predictions are good approximations. The model's predictive abilities rely on binary interaction parameters and it has been observed that some parameters are temperature-dependent. Through the study of binary systems such as ethylene-polyethylene and hexane-polyethylene the binary parameters can be adjusted and then employed in a ternary system simulation to predict the necessary concentration [1]. In systems for which the heat and mass transfer resistances do not influence monomer concentration and temperature within the particles, it was observed that the monomer concentration at the active sites is determined by the equilibrium sorption of the monomer in the polymer particles.

Bashir et al.[3] used Sanchez-Lacombe to predict solubility data in the system ethylene/1-

hexene/LLDPE at 70, 90 and 150°C and found that the predictions were in agreement with experimental data. It was also observed that the solubility improvement depends on the co-monomer.

Alizadeh [1] applied the Sanchez-Lacombe model to the ternary system of ethylene/n-hexane/Polyethylene to predict the change in ethylene solubility in the amorphous phase of the polymer. The predictions were made by fitting the model to the experimental data presented in [12] and adjusting the binary interaction parameters.

3. Model Implementation
3.1. Particle Size Distribution Model

The following assumptions were made when developing the model:

- All active sites on the catalyst have the same propagation constant;

- The concentration of active sites is uniform throughout the catalyst and polymer particles;

- The catalyst possesses only stable active sites that do not suffer deactivation;

- The catalyst particle shape is considered to be a sphere;

- Each catalyst particle is followed individually throughout the reactor;

- The reactors in the battery behave as ideal CSTRs, as shown by their RTD;

The following equation calculates the volume of the polymer particle exiting the reactor:

$$V_p = V_p^0 + \Delta V_p \qquad (3)$$

where V_p is the particle volume, V_p^0 is the catalyst particle volume and ΔV_p is the increase in volume gained through polymerization. In terms of particle diameter this can be translated as:

$$\frac{\pi D_p^3}{6} = \frac{\pi D_p^{0^3}}{6} + \frac{\pi D_p^{0^3}}{6} \frac{k_p[M][C_0^*]\, t\, m}{\rho_{pol}} \qquad (4)$$

where D_p is the particle diameter, D_p^0 is the catalyst particle's diameter, k_p is the kinetic propagation constant, $[M]$ is the concentration of monomer at the active sites, C_0^* stands for the concentration of active sites on the catalyst, m represents the average molecular weight over all co-monomers, t represents the polymerization time and ρ_{pol} is the produced polymer density.

Rearranging equation 4:

$$D_p = D_p^0 \sqrt[3]{1 + \alpha t} \qquad (5)$$

$$\alpha = \frac{k_p[M][C_0^*]\, m}{\rho_{pol}} \qquad (6)$$

The number-based PSD $F(D_p)$ can be related to the reactor RTD $E(t)$ through the expression:

$$F(D_p) = E(t) \left(\frac{dD_p}{dt}\right)^{-1} \qquad (7)$$

By replacing the RTD for a series of n CSTR of equal mean residence times the following equation is obtained:

$$F(D_p) = \frac{3(1 + \alpha t)^{2/3}}{\alpha D_p^0} \frac{t^{n-1}}{(n-1)!\,\tau^n} \exp(-t/\tau) \qquad (8)$$

where τ is the mean residence time in the reactor. This equation can only be used if α and τ do not vary between reactors. Otherwise, if the reactors do not have the same τ or if the polymerization conditions differ, equation 8 can be employed for the first reactor in the series but the subsequent reactors are described with the following equations:

$$D_p^i = D_p^0 \sqrt{\left(\frac{D_p^{i-1}}{D_p^0}\right) + \alpha^i t^i} \qquad (9)$$

$$F(D_p) = \frac{3\left[\left(\frac{D_p^{i-1}}{D_p^0}\right) + \alpha t\right]^{2/3}}{\alpha D_p^0} \times$$
$$\times \frac{t^{n-1}}{(n-1)!\,\tau^n} \exp(-t/\tau) \qquad (10)$$

3.2. Gas-Phase Reactor Model

The following assumptions were made when developing the model:

- A single-phase CSTR approach is considered, operating in Steady-State;

- The reactor is approximated to a cylinder;

- 1 gaseous inlet consisting of ethylene, an inert heavy alkane and nitrogen;

- 1 solid inlet consisting of catalyst particles;

- 1 gaseous outlet containing non-reacted ethylene, inert heavy alkane and nitrogen;

- 1 solid outlet containing the polymer phase, consisting of the polymer and catalyst particles with dissolved ethylene and alkane;

- The catalyst particles are considered spherical and mono-dispersed;

- Catalyst activation is considered to be instantaneous;

- Elutriation of solids is neglected;

- The thermodynamic equilibrium is achieved instantaneously and the polymer particles are considered fully mature;

- The polymer is considered fully amorphous;

- Ethylene and ICA solubility dependence on temperature is neglected;

- Nitrogen solubility in the polymer phase and impact on ethylene solubility are neglected;

- Convective heat transfer is considered between the catalyst/polymer particles and the bulk gaseous phase;

- Due to the heat transfer, 2 different outlet temperatures are considered, one for the gaseous outlet and another for the polymer phase outlet;

- No difference in Pressure is considered between reactor inlet and outlets;

The ethylene mass balance in its most general form is written as

$$Q_{Et,in} - Q_{Et,out} - R_p(T,P)\,V_c - Q_{Et,d} = 0 \quad (11)$$

where $Q_{Et,in}$ and $Q_{Et,out}$ are, respectively, the inlet and outlet flowrate, $R_p(T,P)$ stands for the rate of consumption of ethylene in the polymerization reaction, V_c is the volume of catalyst and $Q_{Et,d}$ is the flowrate of ethylene that dissolves into the polymer phase, described by the following equation.

$$Q_{Et,d} = \frac{C_{Et}^P \, M_{Et}}{\rho_{pol}} Q_{PE} \quad (12)$$

where C_{Et}^P is the concentration of ethylene in the polymer phase, M_{Et} is its molar mass, ρ_{pol} is the density of the polymer phase and Q_{PE} is the polyethylene production flowrate.

Similarly to the case of ethylene, the heavy alkane's mass balance is written according to the following equation:

$$Q_{ICA,in} - Q_{ICA,out} - Q_{ICA,d} = 0 \quad (13)$$

$$Q_{ICA,d} = \frac{C_{ICA}^P \, M_{ICA}}{\rho_{pol}} Q_{PE} \quad (14)$$

The difference between the two is that there is no ICA consumption in the reaction. The mass balance for nitrogen is simple due to the assumptions listed before, and it is written as follows:

$$Q_{N_2,in} = Q_{N_2,out} \quad (15)$$

The mass balance concerning the active sites concentration in the catalyst is essential in accounting for catalyst deactivation. Its main calculated variable is the concentration of active sites after the deactivation has taken place and it is written as follows:

$$Q_c\,C_0^* - Q_c\,C^* - k_d(T)\,C^*\,V_c = 0 \quad (16)$$

where Q_c is the catalyst flowrate, C_0^* is the initial active sites concentration, C^* is the respective concentration after deactivation and $k_d(T)$ is the kinetic deactivation constant, described by the Arrhenius Law.

The polyethylene mass balance starts, of course, with the presentation of the kinetic rate equation assumed. The assumed rate law was proposed by Floyd [7] and is written as follows

$$R_p = k_p\,C^*\,C_{Et}^P \quad (17)$$

where k_p is the kinetic rate propagation constant, described as well by the Arrhenius Law. It is a first order reaction rate law considering a single-site catalyst and takes into account the monomer concentration dissolved in the polymer phase. The polyethylene mass balance is then written through the following expression

$$Q_{PE} = R_p\,V_c\,M_{Et} \quad (18)$$

A simple catalyst heat balance was included in this work to account for the temperature gradient between the polymer particles and the bulk gas phase in the reactor. It is described in the following equation:

$$\Delta H_{polym} = h \cdot A_p \cdot (T_b - T_s) \quad (19)$$

where ΔH_{polym} is the heat released during the polymerization, h represents the convective heat transfer coefficient, admitted by Wong[11], A_p is the particles' heat transfer area and $(T_b - T_s)$ is the temperature gradient between the bulk gas phase and the solid phase, respectively.

Regarding the reactor heat balance, the reference state assumed includes: inlet flow temperature T_{in} as reference temperature; Work Pressure as reference pressure; gaseous ethylene, nitrogen and alkane, solid catalyst and amorphous polyethylene. The balance is then written as follows:

$$
\begin{aligned}
& Q_{Et,out} \cdot \overline{C_{p,Et}} \cdot (T_b - T_{in}) \\
&+ Q_{ICA,out} \cdot \overline{C_{p,ICA}} \cdot (T_b - T_{in}) \\
&+ Q_{N_2,out} \cdot \overline{C_{p,N_2}} \cdot (T_b - T_{in}) \\
&+ Q_{PE} \cdot \overline{C_{p,PE}} \cdot (T_s - T_{in}) \\
&+ Q_c \cdot \overline{C_{p,c}} \cdot (T_s - T_{in}) \\
&+ Q_{Et,reacts} \cdot \Delta H_{polym} = 0
\end{aligned}
\quad (20)
$$

Some diagnostic parameters were also considered to ensure that the reactor operation was within normal boundaries. These parameters were: catalyst

productivity, ethylene per pass conversion and superficial gas velocity.

4. Results

4.1. Particle Size Distribution Model
4.1.1 Validation

The developed model was ran using a MATLAB® script and plotting the results. Validation of the model was achieved by comparing the PSD achieved with the model's script to the PSD presented in reference [9], figure 4, for the same conditions. The results concern a series of 2 CSTR reactors and the comparison is made between the PSD of the particles exiting the 2nd reactor.
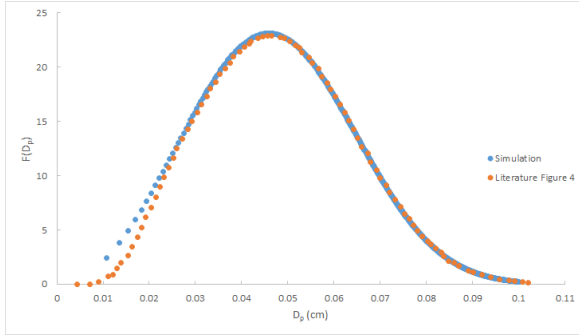

Figure 4: Validation of the model.

By analyzing figure 4 it is possible to see that the model replicates the results presented in the literature[9] with a small deviation at the beginning of the curve. This difference is within the acceptable error and can be explained by the numerical method employed in each circumstance.

4.1.2 Simulation I

Simulation I intends to analyze the effect of catalyst particle diameter on the polymer's PSD.

Table 1: Constant parameters for Simulation I using isobutane as a diluent.

	i		2
τ_1	60 min	τ_2	120 min
k_p^1	1.2 x 10^4 L/(mol.min)	k_p^2	2.4 x 10^5 L/(mol.min)
m	28.05 g/mol	C^*	1 x 10^{-3} mol/L
$[M]$	4 mol/L	ρ_{pol}	915 g/L

The following figure (5) shows the result of the simulation.
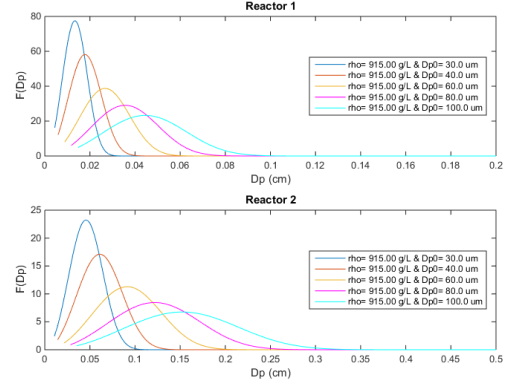

Figure 5: Simulation I polymer PSD results using isobutane as diluent.

A significant difference is detected when varying the catalyst particle diameter (D_p^0). As the diameter increases a broadening of the PSD is observed. This entails an increase in mean particle diameter, as is expected, due to the fact that the polymerization begins with a bigger particle.

4.1.3 Simulation II

Simulation II analyses the effect of polymer swelling on polymer PSD. In this simulation the density of the polymer phase is varied and the monomer concentration as well, due to the fact that they are both predicted by the Sanchez-Lacombe thermodynamic model and represent an equilibrium of the components in the reactor operating at a certain pressure.

Table 2: Constant parameters for Simulation II using isobutane as a diluent.

i	2	D_p^0	30 μm
τ_1	60 min	τ_2	120 min
k_p^1	1.2 x 10^4 L/(mol.min)	k_p^2	2.4 x 10^5 L/(mol.min)
m	28.05 g/mol	C^*	1 x 10^{-3} mol/L

Table 3: Simulation II relationship between total reactor pressure and polymer density and ethylene concentration.

P (bar)	3	5	10	15	18	20
ρ_{pol} (g/L)	823.25	818.96	807.05	792.43	781.46	772.48
$[M]$ (mol/L)	0.0120	0.0206	0.0403	0.0678	0.0892	0.1074

Simulation II analyzes one of the main objectives of this model, effect of particle swelling in polymer PSD. The various simulations were ran for different density and monomer concentration, each corresponding to a different experiment ran at various reaction pressures as mentioned before.In table 3 the data presented concerns the Sanchez-Lacombe EOS predictions for polymer density and monomer

concentration at the active sites for each reaction pressure. The results of the simulation are presented in the following figure 6.
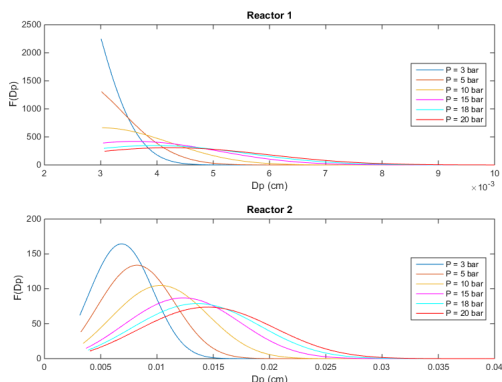

Figure 6: Simulation II polymer PSD results using isobutane as diluent.

Analyzing the PSD of the second reactor the results reflect that an increase in reactor pressure (in other words, a decrease of polymer density combined with an increase of monomer concentration at the active sites) causes a broadening of the PSD resulting, expectedly, in the production of larger particles. In the case of the most swollen polymer ($\rho_{pol} = 772.48$ g/L) the average particle diameter is approximately 150 µm while for the case of the least swollen polymer ($\rho_{pol} = 823.25$ g/L) it is approximately 70 µm.

However, it is clear that by changing reactor pressure, both polymer density (ρ_{pol}) and monomer concentration at the active sites ($[M]$) change. Thus, it is interesting to analyze the effect of polymer density alone on the PSD. To that effect the same simulation was ran with a constant monomer concentration $[M]$ of 4 mol/L and the results are shown in the following figure 7.
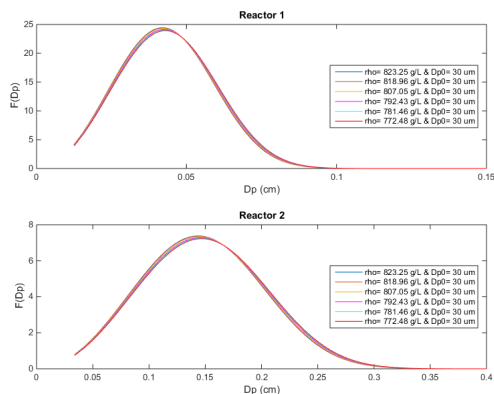

Figure 7: Simulation results varying only polymer density.

Figure 7 shows almost overlapping PSD curves, thus, a magnification is shown in the following figure. The number of curves is also reduced in order to better analyze the differences.
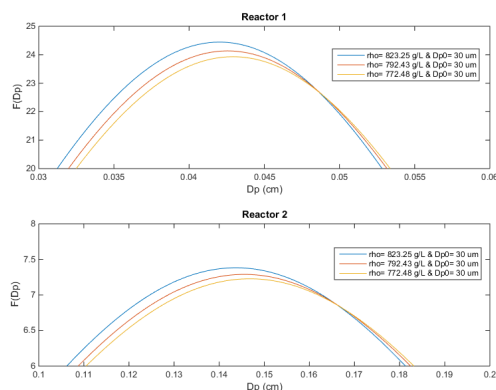

Figure 8: Magnification of the simulation results varying only polymer density.

The results show that a change in polymer density alone does not influence the polymer PSD significantly. It is possible to observe in figure 8 that by decreasing the polymer density from 823.25 g/L to 772.48 g/L the average particle diameter shows a very slight increase from approximately 1.437 mm to 1.468 mm. In other words, a decrease of 50.77 g in a dm^3 (or liter) of polymer only shows an increase of 2% in average particle diameter.

4.1.4 Simulation III

Simulation III analyzes the effect of diluent type on particle swelling and polymer PSD. As such, the simulation was ran based on experiments conducted at the same operating conditions: 90 °C temperature, 3 bar total reactor pressure and 5 % molar concentration of ethylene in the gas phase. The parameters kept constant are the same as those used in Simulation II. The following table summarizes the different conditions obtained for each of the diluents.

Table 4: Parameters obtained for the diluents isobutane and n-hexane, in Simulation III.

Diluent	isobutane	n-hexane
P (bar)	3	3
T (°C	90	90
[M] (mol/L)	9.5×10^{-3}	3.86×10^{-2}
ρ_{pol} (g/L)	814.3	773.1

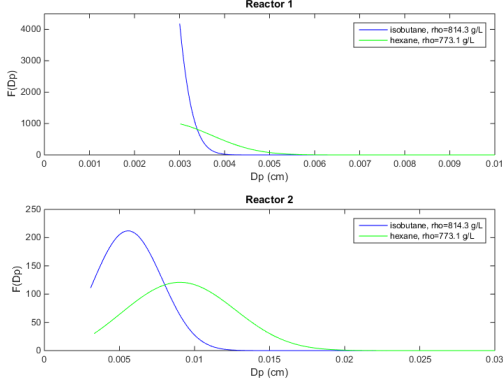The following figure 9 shows the results of this simulation.

Figure 9: Simulation III results. Comparison between isobutane and n-hexane as diluents.

Figure 9 shows that n-hexane causes significantly more swelling than isobutane as shown by its average particle diameter: 56 µm for isobutane and 91 µm for n-hexane.

These results are expected due to the fact that the values predicted by Sanchez-Lacombe indicate a higher monomer concentration near the active sites for n-hexane. This entails a higher polymerization rate and thus, higher productivities (longer chains and bigger particles; more polymer). On the other hand, a higher monomer concentration means that more monomer will be solubilized in the growing polymer phase, further swelling the particles and decreasing the resulting polymer phase density.

4.2. Gas-Phase Reactor Model
4.2.1 Validation

The validation of the developed model is achieved by attempting to reproduce example 7 of US Patent 6864332 B2 [4]. Taking into account the model assumptions described earlier, the most important data assumed for the simulations is summarized in the following table 5.

Table 5: Data assumed for gas-phase reactor model simulation [10, 1, 11, 6, 4, ?].

Parameter	Units	Value	Reference
Inlet Flow Temperature T_0	°C	35	[4, 5]
Inlet Molar Flowrate F	mol/s	11000	Assumed
Reactor Diameter d	m	4.75	[4, 2]
Reactor Bed Height h_b	m	13.3	[4, 5]
Catalyst Particle Diameter d_c	µm	50	[10]
Polymer Particle Diameter d_p	µm	500	[10]
Initial Catalyst Active Site Concentration C_0^*	mol/m³$_c$	0.52	[1]
Heat Transfer Coefficient h	W/(m².K)	280	[11]
Catalyst Density ρ_c	kg/m³	2300	[1]
Catalyst Heat Capacity $C_{p,c}$	J/(kg.K)	2000	[1]
Catalyst Mass Flowrate Q_c	kg/s	0.0019	Assumed
Polymer Heat Capacity $C_{p,p}$	J/(kg.K)	2000	[1]
Kinetic rate constant $k_p^{80°C}$	m³/(mol.s)	180	[1]
Catalyst deactivation rate constant $k_d^{80°C}$	s⁻¹	1 x 10⁻⁴	[1]
Reaction Activation Energy E_a	J/mol	42000	[1]
Catalyst Deactivation Energy E_d	J/mol	42000	[1]
Heat of Reaction ΔH_{pol}	J/mol	-107600	[1]
Fluidized Bed Porosity ε_f	-	0.55	[6]
Total Reactor Pressure P	bar	22.4	[4]
Ethylene Partial Pressure P_{Et}	bar	7	[1]

The example used to validate the model was example 7b from US Patent 6864332 B2 [4]. In this case the reactor is operated in dry mode using ethane at total reactor pressure of 22.4 bar and 35% ethylene molar composition. The alkane chosen to run this simulation was isobutane (partial pressure of 1 bar) and an ethylene molar composition of 31.3 % was achieved under the same reactor pressure. The following table 6 shows the comparison between the results presented in [4] and the results obtained in the simulation.

Table 6: Comparison between results of example 7b of [4] and the results of the developed model simulation.

Parameter	Literature	Simulation	Variation (%)
HDPE Production (t/h)	21.6	21.4	-0.9
Reactor Temperature (°C)	88	88	0
Superficial gas velocity (m/s)	0.75	0.82	9.3

The developed model could be simulated through one of two different methods. The first is a *Microsoft Excel*® workbook using the *Solver* function, where the selected solver must be the GRG Nonlinear solver, since the model is a non-linear system. The second method is a script developed using the software *Matlab*®, more specifically the *fsolve* function of Matlab's Optimization toolbox.

Analyzing the results presented in table 6 it is evident that the developed model is an adequate approximation of reality. The slight difference in HDPE production can be explained by the fact that the reactor inlet compositions are very different in the two cases. The difference of 9.3 % in superficial gas velocity can also be explained by the difference in inlet composition. By considering components with lower heat capacity in the model, the result is that, to achieve the same reactor temperature of 88 °C it is necessary to increase the total molar inlet flowrate F, thus resulting in a higher superficial gas velocity, albeit within the limits of FBR operation.

4.2.2 Simulation I

Simulation I analyzes the effect of increasing n-hexane partial pressure in polyethylene production and reactor behaviour. The parameters used for the simulation were the same ones described in table 5.

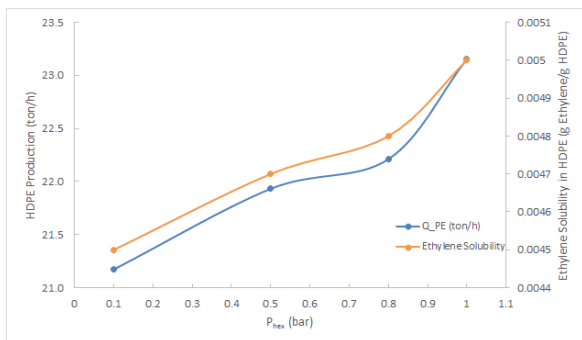The following figures summarize the results obtained from simulation I.

Figure 10: Simulation I HDPE production flowrate results.

In figure 10 it is possible to observe an evident increase in HDPE production with the addition of more n-hexane. The presence of more n-hexane inside the reactor increases the solubility of ethylene in HDPE and, thus, the ethylene concentration near the catalyst active sites.
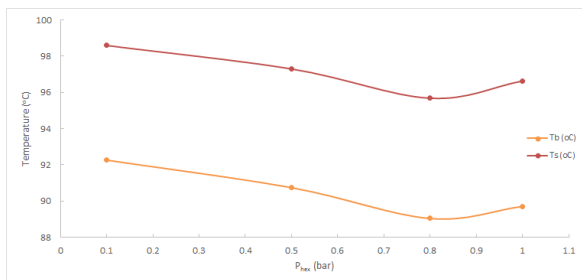

Figure 11: Simulation I bulk and solids temperature results.

In this figure a tendency to decrease both bulk and solids temperature (T_b and T_s, respectively) is expectedly observed, due to the fact that the increase in n-hexane partial pressure also increases the gas stream heat capacity. However a slight temperature increase is observed from 0.8 bar to 1 bar. This increase is explained by the ethylene solubility values predicted by Sanchez-Lacombe EOS (shown in figure 10). Changing n-hexane partial pressure from 0.8 bar to 1 bar Sanchez-Lacombe predicts a steeper increase in ethylene solubility than the ones observed in lower n-hexane pressures. This leads to an value of HDPE production of such an order that the increase in gas mass flowrate is not enough to further decrease the reactor temperature.

4.2.3   Simulation II

Simulation II analyzes the effect of increasing isobutane partial pressure in polyethylene production and reactor behaviour. The parameters used for the simulation were the same as described in table 5 and isobutane pressure was varied from 1 to 13 bar. However, the reactor temperature T_b achieved for 13 bar isobutane is 69.3 °C. The vapor pressure of isobutane at 69.3 °C is 10.7 bar. As such, the reactor is not operating in dry mode. To remedy this the inlet molar flowrate F was corrected to the value of 8000 mol/s and the results of the new simulation are presented in the following figures:
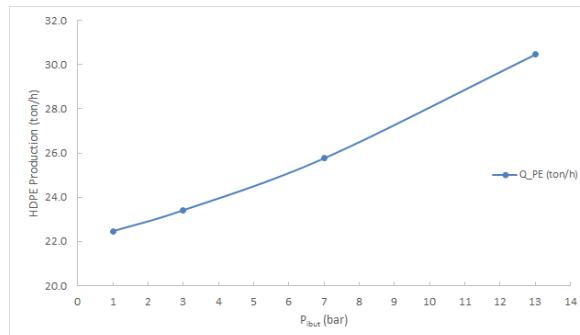

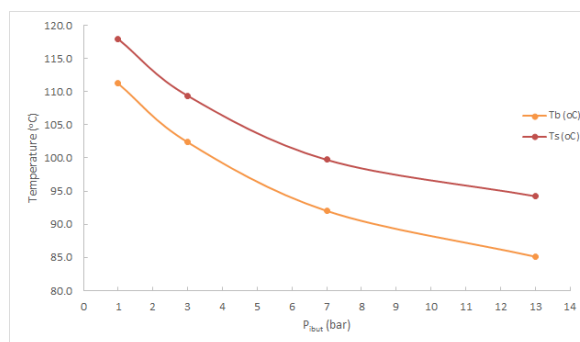Figure 12: Simulation II HDPE production flowrate results.

Figure 13: Simulation II bulk and solids temperature results.

The overall trends observed in this simulation are similar to those observed in Simulation I. The differences between the two are the higher values obtained using isobutane, essentially due to its higher vapor pressure, thus allowing to introduce a greater quantity of alkane while still guaranteeing dry mode operation.

4.2.4   Simulation III

Simulation III compares the results for isobutane and n-hexane in simulations I and II ran under the same conditions. These conditions are: 22.4 bar total reaction pressure, 1 bar isobutane/n-hexane partial pressure and an inlet molar flowrate F of 8000 mol/s. The pressure chosen is 1 bar because the vapor pressure of n-hexane at certain conditions is a restraint for dry mode operation. The results comparison is summarized in the following table:

9

Table 7: Simulation III results. Comparison between n-hexane and isobutane.

Parameter	Units	n-hexane	isobutane
HDPE Production Q_{PE}	ton/h	24.3	22.5
Bulk Temperature T_b	$^\circ$C	112.7	111.2
Solids Temperature T_b	$^\circ$C	120.0	117.9
Productivity	$g_{HDPE}/g_{catalyst}$	3550	3285
Per Pass Conversion	%	9.6	8.9
Superficial gas velocity u_g	m/s	0.633	0.630

Analyzing the results presented in table 7 it is evident that for the same operating conditions (including component partial pressure) n-hexane presents better production results than isobutane, due to a stronger co-solubility effect. In terms of temperature (T_b and T_s), however, isobutane is able to achieve slightly lower temperatures than n-hexane. These results are once again related to the Sanchez-Lacombe predictions of ethylene solubility in HDPE. Ethylene presents a higher solubility in the presence of n-hexane, thus increasing polymerization rate and the amount of heat released. Despite the higher heat capacity, the gaseous stream is not able to absorb enough heat to achieve lower temperatures than isobutane.

5. Conclusions

From the results obtained from the PSD model simulations it is possible to conclude that the parameters that most affect the polymer PSD are kinetic parameters such as the monomer concentration. The increase in these parameters increases the rate of polymerization and bigger particles are produced. The polymer density itself does not significantly affect polymer swelling, especially taking into account the usual density ranges for polyethylene. Diluent type is also a very important parameter that affects polymer swelling, as seen in simulation III.

From the results of the gas-phase reactor model it is possible to conclude that greater quantities of inert alkane increase HDPE production and decrease reactor temperature. Comparing n-hexane to isobutane it is also possible to conclude that, for the same alkane pressure, n-hexane achieves higher productions. However, a comparison between the vapor pressure of the two components shows that it is possible to introduce greater quantities of isobutane than n-hexane, thus effectively achieving higher values of production and lower reactor temperatures.

References

[1] A. Alizadeh. *Study of Sorption, Heat and Mass Transfer During Condensed Mode Operation of Gas Phase Ethylene Polymerization on Supported Catalyst*. PhD thesis, Queen's University, July 2014.

[2] Y. e. a. BANAT. Olefin gas phase polymerisation, Mar. 2014.

[3] M. A. Bashir, M. A.-h. Ali, V. Kanellopoulos, and J. Seppala. Modelling of multicomponent olefins solubility in polyolefins using sanchezlacombe equation of state. *Fluid Phase Equilibria*, 358:83–90, November 2013.

[4] A. e. a. BRAGANCA. Patent us 6864332 b2, process for the gas phase polymerization and copolymerization of olefin monomers, Mar. 2005.

[5] D. BRAGANCA. Process for the gas phase polymerization and copolymerization of olefin monomers, Nov. 2004.

[6] H. Farag, M. Ossman, M. Mansour, and Y. Farid. Modeling of fluidized bed reactor for ethylene polymerization: effect of parameters on the single-pass ethylene conversion. *International Journal of Industrial Chemistry*, 4(1), December 2013.

[7] S. Floyd, K. Y. Choi, T. W. Taylor, and H. W. Ray. Polymerization of olefins through heterogeneous catalysis. iii. polymer particle modelling with an analysis of intraparticle heat and mass transfer effects. *Journal of Applied Polymer Science*, 32(1):2935–2960, July 1986.

[8] A. J. Peacock. *Handbook of Polyethylene: Structures: Properties and Applications*. CRC Press, 1st edition, 2000. ISBN-10: 0824795466.

[9] J. B. Soares and A. E. Hamielec. Effect of reactor residence time distribution on the size distribution of polymer particles made with heterogeneous ziegler-natta and supported metallocene catalysts. a generic mathematical model. *Macromolecular Theory and Simulations*, 4(6):1085–1104, November 1995.

[10] J. B. P. Soares and T. F. L. McKenna. *Polyolefin Reaction Engineering*. Wiley-VCH, 1st edition, 2012. Print ISBN: 978-3-527-31710-3.

[11] Y. S. Wong and P. K. Seville. Single-particle motion and heat transfer in fluidized beds. *AIChE Journal*, 52(12):4099–4109, December 2006.

[12] W. Yao, X. Hu, and Y. Yang. Modeling solubility of gases in semicrystalline polyethylene. *Journal of Applied Polymer Science*, pages 1737–1744, 2007.

[13] K. Yoshio. Global outlook of polyolefin business. Sumitomo Chemical (Asia Pacific) Pte Ltd, September 2011.